Integrating computational biology and forward genetics in *Drosophila*

Sven Vilain*[1,2,3], Shu Hu *[1,2,3], Stein Aerts*[1,2], Leon-Charles Tranchevent*[4], Roland Barriot[4], Jiekun Yan[1,2], Yves Moreau[4], Bassem A. Hassan[1,2,3,#], and Xiao-Jiang Quan*[1,2]

[1] Laboratory of Neurogenetics, Department of Molecular and Developmental Genetics, VIB, Leuven, Belgium.

[2] Department of Human Genetics, K.U. Leuven School of Medicine, Leuven, Belgium.

[3] Doctoral Program in Molecular and Developmental Genetics, K.U. Leuven School of Medicine, Leuven, Belgium

[4] Department of Electrical Engineering, K.U. Leuven, Leuven, Belgium

* These authors contributed equally to this work.

[#] Correspondence: Bassem A. Hassan (Bassem.Hassan@med.kuleuven.be)

Running title: Genetomics of neural development in *Drosophila*

Summary

Genetic screens are powerful methods for the discovery of gene-phenotype associations. However, a systems biology approach to genetics must leverage the massive amount of "omics" data to enhance the power and speed of functional gene discovery *in vivo*. Moreover, few computational methods for gene function prediction have been rigorously tested for their performance on a genome-wide scale *in vivo*. In this work, we demonstrate that integrating genome-wide computational gene prioritization with large-scale genetic screening is a powerful tool for functional gene discovery. To discover genes involved in neural development in *Drosophila,* we extend our strategy for the prioritization of human candidate disease genes to functional prioritization in *Drosophila* . We the integrate this prioritization strategy with a large-scale genetic screen for interactors of the proneural transcription factor Atonal using genomic deficiencies and mutant and RNAi collections. Using the prioritized genes validated in our genetic screen, we describe a novel genetic interaction network for Atonal. Lastly, we prioritize the whole *Drosophila* genome and identify candidate gene associations for ten receptor signaling pathways. This novel database of prioritized pathway candidates, as well as a web application for functional prioritization in *Drosophila*, called HIGHFLY, and the Atonal network, are publicly available resources.

Introduction

The demand by systems biology for *bona fide*, *in vivo* validated, biochemical interaction data and high quality functional annotations is much higher than the supply that geneticists are able to provide, principally because genetic approaches mainly focus on generating data on a gene-by-gene basis. On the other hand, computational predictions of gene function alone remain far from being accurate enough to be considered high-quality biological data. Integrated solutions, that combine the advantages of several approaches, should in theory provide both fast and physiologically relevant genetic data, while simultaneously increasing our understanding of biological processes. Genetic interactions in model organisms constitute a potentially invaluable source of *in vivo* interaction data for systems biology provided that throughput and speed can be increased. Currently, the number of known genetic interactions remains much smaller than the number of annotated physical interactions. For example, the BioGrid database currently contains approximately 37,000 genetic interactions compared to almost 125,000 physical interactions.

Clearly, the power of genetic approaches is that they produce - by definition - data that is directly relevant in a living system. Genetic screens, either for specific phenotypes or for modifiers of gene function, are thus a valuable source of large-scale interaction data. However, the main disadvantage of large-scale genetic screens is that they are costly, labor intensive, and time consuming. Turning *in vivo* genetic screens into a staple of systems biology by making them easier and faster without compromising their accuracy would therefore represent a major advance.

In the bioinformatics community, process- or disease-related genes are, as of recently, being computationally predicted by taking advantage of the large amount of available sequence, function, annotation, and interaction data (Adie et al., 2006; Aerts et al., 2006; Freudenberg and Propping, 2002; George et al., 2006; Lopez-Bigas and Ouzounis, 2004; Ma

et al., 2007; Oti et al., 2006; Perez-Iratxeta et al., 2007; Rossi et al., 2006; Tiffin et al., 2006; Tiffin et al., 2005; van Driel et al., 2005). However to our knowledge, none of these methods have been used in combination with large-scale genetic experiments. Therefore, it remains unclear to what extent genome-wide, or even large-scale, computational predictions of gene-gene or gene-pathway associations, are biologically meaningful. Carrying out such screens on a large scale is difficult in human or mouse genetics, but the availability of genetic tools in *Drosophila melanogaster* together with collections of deficiency lines, mutants, and insertion lines, makes it an ideal model organism to investigate the concept of integrating genetic screens with gene prioritization methods.

Here, we integrate genetics and computational biology to identify genetic interactions underlying neural development in the *Drosophila* Peripheral Nervous System (PNS), a well-established model for neurogenesis. Proneural genes encoding proteins of the basic-helix-loop-helix (bHLH) super-family of transcription factors are essential for the initiation of neuronal lineage development in all species (Anderson, 1999; Brunet and Ghysen, 1999; Campuzano and Modolell, 1992; Guillemot, 1999; Jan and Jan, 1994). They act by forming heterodimers with the widely expressed bHLH E-proteins to bind a DNA motif called the E-box (Cabrera and Alonso, 1991) and regulate the transcription of target genes. The highly conserved members of the Atonal (Ato) family are one example of proneural genes whose activity is required for the development of multiple lineages in vertebrates and invertebrates (Guillemot, 1999; Hassan and Bellen, 2000; Quan and Hassan, 2005; Vervoort and Ledent, 2001). Despite a solid understanding of when and where *ato*-like genes are required in the *Drosophila* PNS and how they interact with Notch signaling to select neural precursor cells (NPCs), the mechanisms that mediate their activity within NPCs and their specificity in inducing neuronal differentiation remain largely obscure.

To demonstrate the power of an integrated approach that combines computational biology and forward genetics - or Genetomics (Hiesinger and Hassan, 2005) - and identify genes involved in *ato* mediated neural development we perform a computationally-supported genetic modifier screen in the *Drosophila* PNS. At the computational level, we propose a strategy specifically oriented to functional gene prioritization in *Drosophila* called HIGHFLY derived from the same principle as the human gene prioritization method ENDEAVOUR (Aerts et al., 2006). HIGHFLY uses both generic and fly-specific data sources to perform its prioritizations, including Gene Ontology annotations, literature data from PubMed abstracts, protein sequences, InterPro protein domains, microarray expression data, genetic interaction data from FlyGrid, gene expression data from *in situ* hybridizations, and phenotypic data from FlyBase. Using this approach to identify the genetic interaction network of the Atonal proneural transcription factor, we develop our integrative strategy combining gene prioritization and genetic screening in several steps. First, HIGHFLY is validated both *in silico* by cross-validations and *in vivo* by comparing the computational output with the results from a pilot small-scale screen of 100 genes for Atonal interactors. Second, genetic tools are used to identify chromosomal loci that, when deleted, dominantly modify the gain of function of *ato*. Third, HIGHFLY is used to prioritize the genes within the positive loci and select a set of candidate genes. Fourth, genetic tools are used again to assay the highest-ranking candidate genes *in vivo* and evaluate the positives for their expression pattern and their specific genetic interactions with *ato* in an *ato* loss of function context. Using this integrated approach we identify 19 genes that interact with *ato* in two different contexts, including 3 previously uncharacterized genes, and use them to predict the core Ato interaction network. Furthermore, to broaden our strategy to other developmental processes, we prioritize the entire *Drosophila* genome for each of ten canonical biological pathways namely, Wnt, TGF-β, Toll, Notch, EGFR, FGFR, Smoothened, Hedgehog, JAK-STAT and Sevenless and

demonstrate that these prioritizations match well with genome-wide siRNA screens for several pathways. Based on this, we generated a database of candidate members or interactors for each pathway. This novel database of pathway candidates, as well as the HIGHFLY web application and the novel Atonal genetic interaction network, are freely accessible community resources at http://med.kuleuven.be/cme-mg/lng/HIGHFLY.

Results

Identifying modifier loci of *atonal*-induced neurogenesis in the *Drosophila* PNS

Three amino-acids within the basic domain of the first helix have been shown to mediate the specificity of *ato* function (Quan et al., 2004), and the same motif enables specific transcriptional activation of the nicotinic acetylcholine receptor beta-3 subunit by the *ato* orthologue Ath5 (Skowronska-Krawczyk et al., 2005). Substituting the same amino acids in the Ato-related mouse proneural protein Neurogenin 1 (Ngn1) for Ato group-specific residues (Ngn^{bAto}) allows Ngn1 to induce neurogenesis in *Drosophila*. This induction mimics that caused by Ato itself and depends on the fly E-protein Daughterless (Da) and the proneural co-factor Senseless (Sens). Also, like endogenous proneural activity, it is antagonized by the Notch signaling pathway. Expression of the "Atonalized" form of mouse Ngn1, Ngn^{bATO} (Figure 1A) under the control of *dpp-Gal4* induces an average of ~30 ectopic sensory bristles on the adult wing vein (n= 30; Figure 1B, C). This is in contrast to an average of only ~7 bristles induced by Ngn1 itself (n=26; $p<0.001$), but is similar to the number induced by Ato (n=26, n.s.; Figure 1C). However, unlike Ato, Ngn^{bATO} induces significantly less lethality and many fewer wing deformities making it much easier to use in a large scale, quantitative genetic screen. In addition, just like Ato, removal of one copy of *sens* reduces the number of Ngn^{bATO}-induced bristles by 55.6% (Figure 1C). In order to bring the screen to a dosage critical value, a heterozygous *sens* mutant was introduced into the background of *UAS::*Ngn^{bATO}*; dpp-Gal4*. The number of ectopic bristles with this system provides a sensitized and quantitative read out in which to screen for modifiers of Ato function.

To test the feasibility of isolating dominant modifiers of the number of ectopic bristles, we crossed *UAS::*Ngn^{bato}*/Cyo;sens,dpp-Gal4/TM6c*, flies to *da* or *Notch* mutant flies. We find that removal of a single copy of *da* almost completely suppressed Ngn^{bATO} induced bristle formation (average of 0.7 ± 0.9 bristles; n= 27, $p<0.001$), while removal of one copy

of Notch strongly enhanced the phenotype (average of 43.5 ± 4.1 bristles; n=23, p=0.002; Figure 1C). All together, these data suggest that the assay is both robust and sensitive and should enable the identification of genes involved in *ato*-dependent neurogenesis in the *Drosophila* PNS.

Following this strategy, a deficiency screen of the second and the third chromosomes for modifiers of Ngn^{bato} misexpression was performed. The deficiency kit is a collection of fly stocks that each carries a deficiency, or deletion, chromosome uncovering multiple genes. The different deficiencies encompass most of the chromosome and deficiency screening is an established and rapid assay to identify chromosomal regions with enhancer and suppressor loci for a give phenotype or pathway (St Johnston, 2002). To identify chromosomal loci that influence *ato*-induced neural development, 180 deficiency fly lines were crossed to *UAS::*Ngn^{bato}*/Cyo;sens,dpp-Gal4/TM6c*, flies. Loci were considered positive if they altered the number of ectopic bristles on the adult wing vein by more than a cut-off of 30% compared to the number of bristles induced in sibling control flies, as well as in wild type Canton S flies, and if the change in bristle number was strongly statistically significant ($p<0.01$). Following these stringent criteria, 17 positive regions on chromosome 2 and 14 positive regions on chromosome 3 were identified. Since induction of ectopic bristles is a common property of all proneural genes, the identified loci might be involved in both *achaete-scute* and *ato* dependent neurogenesis. In order to identify Ato-specific loci, the individual candidate deletion stocks were tested with flies expressing *UAS::ato, UAS::ngn1,* and *UAS::sc*, respectively, under the control of *dpp-Gal4*. The loci which modified Ato misexpression, but not that of Sc or Ngn1 were considered to be Ato-specific loci. Of the 31 loci identified in the primary screen, only one failed to interact with any of the genes in the secondary screen. We find that 15 of the 31 loci interact with both *ato* and at least one other proneural gene, while 2 loci interact only with *ngn1* and 1 locus interacts only with *sens* (data

not shown). The remaining 12 loci (6 on chromosome 2 and 6 on chromosome 3) interact specifically with *ato*. Examining the breakpoints of the overlapping deletions uncovering these 12 loci shows that they harbor 1122 annotated genes (Figure 1D). Each of these loci is expected to harbor one or more *ato*-interacting genes.

The identification of the individual modifier genes from these regions is similar to the problem in human genetics where for a given human phenotype and its underlying chromosomal locus, identified by cytogenetic studies or linkage mapping for example, the individual disease-causing gene(s) need(s) to be identified. Besides directly providing interaction candidates, the twelve positive regions resulting from the deficiency screen provide an excellent opportunity to test the principle of gene prioritization on a large scale and in an unbiased setup. First we present a novel implementation of a gene prioritization approach that is specifically tuned towards the *Drosophila* genome, and then we use it to select the most promising candidates from the 1120 genes within the twelve positive regions.

HIGHFLY: a tool to prioritize *Drosophila* genes through genomic data fusion

To prioritize *Drosophila* genes we implemented a tool- henceforth referred to as HIGHFLY- based on the concept of genomic data fusion and the Endeavour human gene prioritization tool (Aerts et al., 2006). The method works as follows. First, a set of training genes is defined to describe the particular process under study. For each data source, the following data for the training genes are collected: sequence, expression profiles, functional and pathway annotations, phenotypes, literature references, and interaction partners. Each data type is then summarized across the training set, generating a submodel. Next, the test genes are scored and ranked according to each individual submodel. Finally, all rankings are integrated using order statistics to yield a final overall rank. In HIGHFLY, the ranking of test genes according to the similarity with the training genes is based on (1) a gene's function

derived from FlyBase GO annotation, textual information extracted from PubMed abstracts, Swissprot keywords and KEGG pathway membership; (2) a gene's expression pattern derived from two general *Drosophila* microarray data sets (Arbeitman et al., 2002); (Li and White, 2003) and embryonic *in situ* expression patterns from the Berkely Drosphila Genome Project (BDGP); (3) a gene's protein sequence by homology to the training set and the presence of similar protein domains from InterPro; (4) described mutant phenotypes in FlyBase; and (5) described genetic interactions or predicted protein-protein associations from FlyGrid and STRING. The applied training and scoring strategies for each data source are described in Table 1.

To test the performance of each individual data source we carried out leave-one-out cross-validations (LOOCV; see below and Experimental Procedures) on several cross-validation sets (i.e., training sets without independent test set where the performance is evaluated by LOOCV). Each cross-validation set contains genes that are related to each other for different reasons: genes involved in the same signaling pathway, tested on eight pathways defined by GO; genes with similar expression patterns using an expression cluster from Arbeitman et al. (Arbeitman et al., 2002) and a second cluster of all genes expressed in Bolwig's organ from FlyBase; genes with the same protein domain, namely the bHLH domain; all genes that interact with the same gene, tested on all interactors with Atonal from FlyGrid; and genes that are co-cited with a specific gene in PubMed abstracts, namely genes cited with *ato*, extracted using iHOP (Hoffmann and Valencia, 2004). In LOOCV, every gene from every validation set is, in turn left out, and the ranking of the left-out gene within a set of 99 randomly selected genes is recorded. From all these rankings, Receiver Operating Characteristic (ROC) curves are generated and the area under this ROC curve is used as a measure of the performance of each individual data source and of the integrated prioritization (Figure 2). Depending on the type of relation between the genes in the training set, several

particular data sources show high individual performances that contribute most to the overall performance. For example, genes that are functionally related, either because they share the same GO annotation or because they co-occur in the literature, are prioritized well with the GO and text submodels, but also with the STRING and FlyGrid submodels. Similarly, prioritization of genetically interacting genes works well with the FlyGrid, STRING, GO and Text submodels. On the other hand, Genes that share similar microarray expression profiles or similar *in situ* expression patterns are prioritized well with their respective submodels. Lastly, genes that share similar protein domains are prioritized best by the InterPro and BLAST submodels. Importantly, regardless of which particular submodels show the strongest performances, the overall performance is highly robust for all sets (i.e., it is not influenced by non-informative data sources) and almost always greater than 90% compared to a performance of ~50% for randomly assembled sets of genes (Figure 2). In conclusion, HighFly ranks highly the correct genes (i.e., left-out in the LOOCV) when at least one data source holds the information that this gene is related to the remainder of the gene set. These results validate the technical aspects of the implementation and suggest that HIGHFLY performs robust prioritizations on *Drosophila* data sources.

Next, we investigated whether HIGHFLY would be capable of finding known and novel genes that interact *in vivo* with *ato*. A training set, called TRAIN_Ato1 was assembled with the following genes: *ato*, *Brd*, *rho*, *Takr86C*, *pnt*, *dpp*, *Egfr*, *da*, *wg*, *sens*, *chn*, and *sca*. The trained GO submodel for this set contains "peripheral nervous system development", "cell fate specification", "eye morphogenesis", "sensory organ development", etc. as highly over-represented terms (p value < 10^{-09}). The Text submodel contains stemmed terms like "cell fate", "notch", "egfr", "disc". The InterPro submodel has no highly over-represented domains, but "Basic helix-loop-helix dimerisation region bHLH" is marginally over-represented (corrected p-value = 0.07). The training set can be downloaded from the

HIGHFLY website (http://med.kuleuven.be/cme-mg/lng/HIGHFLY) to inspect the other submodels and to prioritize the genome or any region of interest. To test the homogeneity of TRAIN_Ato1, we subjected it to LOOCV and obtained an AUC performance of 98.5%, suggesting that TRAIN_Ato-1 is a coherent and internally consistent training set. To test the possibility of obtaining biologically meaningful prioritizations, we performed a pilot test by prioritizing the right arm of chromosome 3 (chr3R) using TRAIN_Ato1 and then divided all the genes on the list into three groups: the top 1/3, the middle 1/3, and the bottom 1/3. From each group the top 30 genes for which stocks with mutant alleles are available from the public stock centers were examined for their modification of *ato*'s proneural activity, using the same bristle induction assay described above. Four positive genes were found in the top group (*rn*, *Antp*, *gro*, and *pros*), none in the middle group, and none in the bottom group (Table 2, top panel). Although the power of this preliminary test is limited due to the relatively small number of genes tested (90), we found these results sufficiently encouraging to proceed with HIGHFLY prioritizations of all twelve modifier loci found in the deficiency screen. However, to further evaluate HIGHFLY, we intentionally chose a less stringent threshold of further validating the top 30% of ranked genes to compare the rankings of positive and negative genes with a sufficiently large sample size at the end of the screen.

Identification of novel *ato* interacting genes through the integration of gene prioritization and functional genetic modifier assays

To identify candidate genes within the positive regions, all genes in each of the twelve positive regions were prioritized using TRAIN_ATO1 as training set and all 12 HIGHFLY data sources. For all genes that were ranked within the top 30%, a mutant stock, when available, was ordered from the public stock centers. Each mutant was then crossed to the sensitized tester fly stock (*uas::ngn*^{bato}*/Cyo;sens,dpp-Gal4/TM6c*) and the bristles at the anterior-

posterior margin (where *dpp-Gal4* is expressed) were counted and compared to the number of bristles observed in the control flies as described above. For twelve genes, namely *toc*, *lilli*, *Sbb*, *fj*, *mus209*, *zip*, *shg*, *Egfr*, *dom*, *smg*, *cas* and *ppan*, the number of bristles was significantly lower or higher ($p<0.01$) than in the control flies (Table 2, bottom panel). Each of these mutants were then tested against *uas::sc/Cyo; dpp-Gal4/TM6c* to check for the specificity of *ato* interaction None of the genes modified the *sc* gain of function phenotype (data not shown). We note that although mutants of genes that ranked in the top 30% of each locus were tested, all positive genes ranked in the top 15% and 10 of the 12 ranked in the top 8% of their locus (Table 2), suggesting that HIGHFLY prioritizations enrich strongly for positive interactions. The contributions of each submodel to the ranking of the positive genes is shown in Figure S3. Similar prioritizations were obtained by using a different high-quality training set (LOOCV AUC=99.5%), assembled by selecting all 18 known interactors of *ato* from FlyGrid (data not shown). In contrast when the same 12 genes were prioritized using 100 randomly assembled training sets, the median rank ratio was 0.247 compared to 0.0392 for the *ato* training set (Figure 3). Functional inspection of the 16 positive genes (12 from the deficiency screen + 4 from the pilot screen of 100 genes on chromosome 3R) by Gene Ontology statistics (Boyle et al., 2004) revealed that this gene set is significantly enriched for developmental processes that require *ato* such as eye development and regulation of transcription (Table 3). Finally, we compared the phenotypic distribution of the effects of the modifier genes identified in our screen with the distribution documented for saturating forward genetic screens and cellular siRNA screens (Friedman and Perrimon, 2007). We find that despite the relatively small number of genes that need to be tested in a HIGHFLY screen, the distribution of phenotypes mirrors that obtained in genome wide forward and reverse genetics screens (Figure 4). These data further support the power and accuracy of the integration of computational biology and genetics.

ato acts as a proneural gene for two different types of founder cells. The first is a subset of sense organ precursor (SOP) of the body wall and appendages and the second is the R8 founder cell of the retina. The major difference between the SOP and the R8 is that the SOP undergoes cell division to generate the sensory organ, whereas the R8 cell terminally differentiates. However, both cells share the property of recruiting neighbouring cells into the *ato*-dependent fate; a property unique to *ato*, not shared by other proneural genes. We assessed whether genes identified in one context, also operate in the other. To this end, we tested the relationship between *ato* and its putative interactors in the developing fly retina, where *ato* function is well described (Jarman et al., 1995). In the retina, *ato* specifies the first photoreceptor, or R cell, the R8 (Figure S1A, B). The R8 then releases an *ato*-dependent EGF signal which organizes the rest of the retinal field and specifies the R1-R7. Loss of *ato* function in the retina results in the complete failure of retinal specification (Jarman et al., 1994). Expression of an *ato-RNAi* construct (A kind gift of A.P. Jarman) in the eye in *ato* heterozygous flies (*uas::ato-RNAi;h-Gal4, ato*^{1}; see experimental procedures) reduces R8 specification and consequently the recruitment of other R cells in a dose dependent fashion (Figure S1C,D). One copy of *ato-RNAi* produces a smaller eye with approximately half the normal number of ommatidia (Figure 5A,B). Mutants for the 16 genes identified in the screen were crossed to the *ato-RNAi* flies and scored for their ability to dominantly modify the *ato* RNAi phenotype. Ten of the 16 tested genes, namely *gro*, *rn*, *EGFR*, *cas*, *ppan*, *toc*, *sbb*, *fj*, *shg* and *dom* dominantly enhanced the *ato-RNAi* phenotype, with nine showing further reductions in eye size to approximately 250 ommatidia (Figure 5C, D). An 11th gene, *pros*, was semi lethal. The remaining five genes, namely *Antp*, *smg*, *lilli*, *mus209*, and *zip*, did not appear to alter the *ato-RNAi* induced small eye size.

The data thus far suggest that at least 10 of the 16 genes we identified in the deficiency screen also interact with *ato* during retina development. Some of these genes such

as *pros* are known for their role in neurogenesis (Vaessin et al., 1991), while the EGF receptor is well known for its close interactions with *ato* (Lage et al., 1997). However, most of the genes we identified as genetic interactors of *ato* have not, to our knowledge, been previously shown to play a role in *ato*-dependent neurogenesis. Next we asked if these genes are co-expressed with *ato* in the various PNS anlagae that derive from *ato* expressing precursors. We were able to obtain LacZ enhancer trap lines from stock centers for 10 of the 16 interacting genes (*dom, fj, lilli, mus209, pros, rn, sbb, shg, toc* and *zip*) to examine their expression patterns in the third instar larval (L3) imaginal discs. In the eye, antennal, leg and wing L3 discs, Ato marks the progenitor pools and the very early precursor cells of specific neuronal lineages. Senseless then marks the precursor cells during and after Ato expression. One gene, *rn*, did not show any obvious expression relationship to *ato*. Two of the 10 genes, *mus209* (fly PCNA) and *sbb* are generally expressed. An additional two genes, *toc* and *zip* showed expression in the posterior part of the eye disc (Figure S2A), suggesting a later function than that of *ato*. Finally, five of the 10 tested genes showed a clear expression relationship with Ato (Figure S2). We observed strong lacZ expression in the L3 discs in Ato-expressing and Ato-dependent cells in the eye disc (*fj*, *lilli*, *shg*, *pros*), in the antennal Johnston organ precursor cells (*dom*, *shg*, *pros*), in the chordotonal organ precursor cells of the wing and leg imaginal disc (*dom*, *shg*, *pros*) (Figure S2 and data not shown).

Identification of uncharacterised *ato* interacting genes.

The data above support the feasibility of rapidly and accurately identifying gene function through the fusion of *in silico* gene prioritization and *in vivo* genetic screens. One issue that faces all gene prioritization approaches is an expected bias towards genes with at least some explicit information in several databases. Although this is still extremely valuable in assigning novel functions to known genes, we reasoned that it would be interesting to test

the performance of HIGHFLY in the prioritization of genes about which there is very little explicit information. Interestingly, many such genes, known only by their CG numbers, ranked in the top 10% of the *ato*-specific deletion loci identified in the initial bristle screen (Table 4). The recent availability of a genome-wide *in vivo Drosophila* RNAi library (Dietzl et al., 2007) allowed us to test these genes for their interaction with *ato*.

When no off-target effects were predicted, available RNAi lines for these genes were ordered and crossed to the *ato-RNAi* flies driven by the *h-Gal4* driver in an *ato* heterozygous background (*uas::ato-RNAi;h-Gal4, ato*^{1}), as well as two different control lines; *h-Gal4, ato*^{1} and *h-Gal4* alone. To avoid potential artifacts resulting from the RNAi approach, we set relatively stringent criteria: we searched for genes that show synthetic lethality specifically and only in combination with *ato-RNAi*, but show no phenotype under the two control conditions.

There are 24 uncharacterized genes ranking in the top 10% of positive deficiency regions, for which we were able to obtain a total of 36 RNAi lines. Eleven RNAi lines were lethal under all conditions and could not be evaluated further. The 25 remaining RNAi lines allowed us to perform knock-down of 17 genes. Of these, 2 genes (*CG1024*, *CG1218*,) caused lethality only in combination with *atoRNAi*, but not under control conditions (Table 5). As a further confirmation for the specificity of these interactions, we tested 51 RNAi lines for the bottom 10% ranking genes in each deficiency. None of these lines showed specific synthetic lethality in combination with *atoRNAi* (data not shown). Thus, the combination of HIGHFLY prioritization, the RNAi library and genetic screening allows the rapid functional identification of previously uncharacterized genes.

An Atonal interaction network

The combination of forward and reverse genetics tools and computational biology allowed the identification of 19, mostly novel, genetic interactions with the proneural gene *ato*. We sought to determine if the identified positive genes are functionally associated with each other, with *ato*, and with any of the other training genes that were used originally to identify these genes. To this end we used the STRING (von Mering et al., 2007) protein association predictions at 0.8 confidence level and determined the optimally connected sub-network that can be formed among the 19 positive genes, via maximally two other proteins. We find that a network can be constructed that includes 13 of the 16 known genes (data not shown). As expected, the 3 unknown genes play no role in this analysis because of the lack of STRING data at this high confidence level. This analysis discovers Ato itself as member of the best network that connects the positive genes. We found that the maximal confidence level at which Ato is still part of the network is 0.842, and therefore used the is stringency for further analyses. The network formed by the 16 known genes at this confidence level (Figure 6A) contains 84 nodes and 250 edges, and now includes 11 of the 16 positive genes and 6 training genes, including *ato*. *fj*, *Antp* and *gro* are connected to *ato* via one other protein; *pros*, *rn*, *shg*, *lilli* are connected to *ato* via 2 other genes and *cas*, *smg*, *zip*, *mus209* via 3 other genes.

To determine the significance of finding a large interconnected network, which includes *ato*, starting from the 16 positive known genes, we generated 1000 random sets of 16 known genes. Specifically, we used only genes with a name in FlyBase and at least one GO biological process annotation. Only 29 of the 1000 networks contain *ato* and, on average, they contain 0.70 (S.D.=1.13) training genes, 7.83 nodes (S.D.=9.09), 13.07 edges (S.D.=19.28). An example of such a network is shown in Figure 6B. With a p-value of 0.029 to find Ato in the real network, $p<0.001$ to obtain 84 nodes, $p<0.001$ to obtain 250 edges, and

p=0.001 to recover 6 of the 11 training genes, we conclude that the positive genes we identified are strongly associated with each other and with Ato and its known interactors.

A database of genome-wide gene prioritizations in *Drosophila* for ten canonical signalling pathways

A particular feature of the HIGHFLY tool is the speed of prioritization. We wondered whether this computational efficiency makes it possible to prioritize whole chromosomes or even the entire genome. To this end we asked if it is possible to rank the 16 known genes identified in our screen on their respective chromosomes, and if so, whether these rankings would be high. Table 2 shows the chromosomal rankings of these genes. All known genes rank within the top 10% of their respective chromosome and all except two genes (*mus209* and *ppan*) rank in the top 4% (Table 2).

These data suggest that it is possible to obtain strongly meaningful gene prioritizations across large data sets. We sought to illustrate the general applicability of fly gene prioritization and simultaneously generate a second community-wide resource by prioritizing the entire genome to identify genes that are related to, or potentially involved in, either of ten signaling pathways, namely Transforming Growth Factor beta (TGFβ) receptor signaling pathway (GO:0007179), Epidermal Growth Factor Receptor (EGFR) signaling pathway (GO:0007173), Fibroblast Growth Factor Receptor (FGFR) signaling pathway (GO:0008543), Notch (N) signaling pathway (GO:0007219), Sevenless (Sev) signaling pathway (GO:0045500), Smoothened/Hedgehog (Smo/H) signaling pathway (GO:0007224), Toll signaling pathway (GO:0008063), Extracellular signal-Regulated Kinase (ERK; GO:0007259), JAK-STAT (GO:00016055) and Wnt signaling pathway (GO:0016055). To investigate the rankings in terms of biological processes we calculated GO over-representations for each top 100 ranked genes, excluding the training genes. We also

excluded genes that were ranked in the top100 for more than two pathways and GO-terms that were over-represented in more than four pathways. We find that typical overrepresented functions are cell adhesion and photoreceptor fate commitment for EGFR-related genes; tube development for FGFR; sensory organ development and equator specification for Notch; defense response for Toll; and wing disc development for Wnt, suggesting that the prioritizations are biologically meaningful. Finally, we compared prioritizations for 4 of the 10 pathways- namely ERK, Wnt, Hh and JAK-STAT- for overlap with published genome-wide siRNA screens. We find significant overlap between the top 10% of the genome as prioritized by HighFly and the genes scored as positives in these screens for 3 of these pathways (Figure 7). Only the Hh pathway screen shows poor overlap with the prioritizations. Prioritizations and functional analyses, as well as the HIGHFLY software, are freely available at http://med.kuleuven.be/cme-mg/lng/HIGHFLY.

Discussion

The molecular unraveling of biological processes in the post-genome era is characterized by the use of high-throughput experiments and the integration of prior knowledge (e.g., the use of GO-statistics to select microarray generated gene clusters), and is therefore supported and guided by bioinformatics. Genetic screens in model organisms such as *Drosophila melanogaster* are also high-throughput experiments, but they are yet to be aided by computational techniques, as an integral part of the screen itself. We sought to demonstrate the power of an integrated approach that combines high-throughput *in silico* and *in vivo* genetic approaches. This integration allowed us to quickly identify novel genetic interactions during neural development in the fly PNS, while significantly reducing the workload of the genetic screen. First, a classical deficiency modifier screen is performed. Then, instead of assaying all the genes located within the positive deficiency regions, the best

candidates are selected computationally. This is done by integrating multiple heterogeneous genome-scale data sources, both representing published knowledge (e.g., functional gene annotations or protein-protein interactions), genome sequences, and experimental data (e.g., gene expression data). As such, we were able to assign novel functions for known genes whose involvement in *ato*-dependent neural development was unknown, as well as describe functions for uncharacterized genes.

A major advantage of genetic screens is that they are unbiased: they can reveal a function for a previously unknown gene. Although gene prioritization based on available data would have been expected to affect this property of screens, our data indicate that this is not necessarily the case. Even genes with very little explicit information, and no known function could be identified both as high ranking and as *bone fide* interactors *in vivo* in our HIGHFLY supported screen. In addition, our data suggest that the combination of HIGHFLY prioritizations and transgenic RNAi lines can result in very rapid functional gene discovery.

The use of an integrative screening strategy combining computational biology with medium or high-throughput screening assays is likely to be applicable to a broad range of screening assays (from *in vitro* to *in vivo* assays) beyond *Drosophila* genetics. Essentially any assay designed around evaluating a given gene, and for which whole-genome screening is outside the reach of the typical lab, could benefit from strategies similar to ours. Even with more extensive resources, it may be more productive (at equal time and cost) to evaluate several prioritized screens than a single-whole genome screen. Obviously, the strategy we propose is not applicable in the case where extremely little is known about the molecular basis of a phenotype (because of lack of a training set) while a genetic screen would still be feasible. It is a clear research challenge for computational biology to develop methods applicable to such a situation.

A further advantage of our integrated systems genetics approach is the combination of speed and accuracy of gene function discovery. In this work we tested a total of 180 deletion lines, 220 mutants and 36 RNAi lines to identify 19 *ato* interacting genes, representing a discovery rate of ~5%. It should be noted that the 220 mutants tested include 100 mutants examined only for the purposes of testing the prioritizations as well as 78 mutants ranking between 10% and 30% of their deletion regions. Our data clearly indicate that testing genes ranked in the top 10% only will suffice to discover the vast majority of sought after genes: 17 of the 19 genes identified (~90%) rank in the top 10% of their deletion regions. Thus, assuming all genes have available RNAi lines or mutant alleles, testing only 96 genes, after the initial deficiency screen, would have identified at least 17 *ato* interacting genes, a discovery rate of almost 18%.

The genes we find to interact with *ato* reveal an interaction network underlying early neural differentiation. Network analysis reveals two important aspects of the screen. Although neither Ato nor its known interactors were included in the query, the best network found includes Ato and almost all of its known interactors. In addition network analysis yields a number of interesting insights. First, most of the 89 genes in this network are signaling molecules and transcription factors belonging to the Notch, Wnt, EGFR, Dpp and Hh pathways. These pathways are known to interact with *ato* and our data suggest that the newly identified *ato* interacting genes may be members of these pathways that implement the interactions between *ato* and these pathways. Second, most of the genes tested for both bristle formation and retinal development interact with *ato* in both assays. This suggests that *ato* may work with a core group of genes- which we may term the Ato toolkit- to implement context-specific neural fate decisions. One exception to this appears to be genes acting in cell division (*mus209, lilli, zip*) which, not surprisingly, interact in the bristle assay, but not the

R8 assay. Third, we note that HIGHFLY was able to predict the interaction of uncharacterized genes with *ato*, which network analysis alone would have not been able to predict.

In summary, a genetomics approach not only identifies novel functions for individual genes with great speed and accuracy, but, as would be desirable in a systems biology context, also uncovers the structure and functional attributes of the network formed by these genes. Yet, the main advantage of systems genetics over other systems biology approaches is that the results are physiologically relevant by definition, because they are discovered directly *in vivo*.

The HIGHFLY tool can perform prioritizations on the entire fly genome. We have done this for ten major signaling pathways, but many other prioritizations are possible, depending on the interest of the user. HIGHFLY and its prioritizations are public resources that we hope will contribute to enhancing the speed and accuracy of functional gene discovery *in vivo* and establishing classical genetics as a fundamental tool of systems biology.

Materials and Methods

Fly strains and genetics

All crosses were performed at 25°C, except for the *atoRNAi* eye screen crosses which were performed at 28°C, on standard fly food. Deficiency kits, *LacZ* enhancer trap flies and all mutant lines were obtained from the Bloomington and Szeged stock centre. The *atoRNAi* lines were kindly provided by Andrew Jarman, and the RNAi lines for uncharacterized genes were obtained from the Vienna *Drosophila* RNAi Center (VDRC).

Immunohistochemistry

Third instar larval imaginal discs were dissected in 1X PBS. Discs were fixed with 4% formaldehyde in 1X PBT for 15 minutes. Then, washed five times (15min/T) in 1X PBT. Blocking and antibody incubation were performed as described [39]. The antibodies used were: mouse anti-β-Gal (Promega, 1:2000), rabbit anti-ATO (1:1000), rabbit anti-GFP (1:1000), rat anti-Elav (1:100), guinea pig anti-SENS (1:1000) mouse anti-βgal (1:1000), rabbit anti--βgal (1:1000). Secondary antibodies were always used 1 in 500. Samples were mounted in Vectashield mounting medium and detected using confocal microscopy (BioRad 1024, Hercules, California, United States and Leica DM-RXA, Wetzlar, Germany)

Genetic screen

The fly strain *w*; *UAS::ngnbato*/*CyO*; *sens*, *dpp-GAl4*/*TM6* was used to set up crosses with deficiency lines. The number of the ectopic bristles was used as a parameter to reflect the strength of the proneural function of Ato in this context [23]. When a deficiency region caused a significant change in the number of ectopic bristles, the corresponding deficiency line was further crossed to three fly lines *UAS::ato; dpp-Gal4, UAS::ngn; dpp-Gal4* and *UAS::sc; dpp-Gal4* and the number of ectopic bristles was counted. Deficiencies were

considered *ato* specific when they altered the amount of bristles generated by *UAS::ato; dpp-Gal4*, and not by *UAS::ngn; dpp-Gal4* or *UAS::sc; dpp-Gal4*. Within these deficiency regions, all mutant lines available in the stock centre were ordered and crossed to *w*; *uas::Ngnbato*/*CyO*; *sens*, *dpp-GAl4*/*TM6*. If a mutant still caused a significant change in bristle number, the corresponding gene interacts with Ato. The positive genes were crossed again to *UAS::sc; dpp-Gal4* to check for specificity. All ectopic bristles were counted under stereomicroscope. And for all statistic analysis, the sample number is n=10, and significant difference between two average values is defined when $P \leq 0.01$. The eye phenotype screen was performed by crossing *w*; *UAS::atoRNAi*/*CyO*; *h-Gal4*, ato^{1}/*TM6C*, which reduced the eye size in 50% of the flies, with the mutant strains identified in the bristle screen, or RNAi lines. Positive genes for retinal modifiers of *ato* were mutants or RNAi lines that enhanced or suppressed the atoRNAi phenotype. RNAi strains were crossed to *h-Gal4*; ato^{1}/*TM6* and *h-Gal4* as controls

Gene prioritization

The implemented gene prioritization system is as follows. For each data source a "submodel" is trained based on a set of "training genes". Attribute-based data (GO, KEGG, InterPro, BDGP *in situ* expression data, FlyBase phenotypes, and Swissprot keywords) are summarized by over-representation p-values. For each gene in a "test set" the similarity with the submodel is calculated and the individual submodel scores are then integrated using order statistics, yielding a q-value. The q-value is transformed into a p-value according to fitted distributions, depending on the number missing values. Finally, the test genes are ranked according to this p-value. The data sources are described in Table 1, together with the training and scoring procedures for each submodel type.

Network extraction

The aim of the network extraction is to obtain a subgraph that connects the genes of interest (the seed genes). Network connections were extracted from the STRING protein-protein associations, using a minimum edge confidence (above 0.8). We define the connecting nodes (the non seed genes) in the subgraph as the nodes that are on the shortest path(s) between two or more seed genes. To identify those connecting nodes, a multiple sources breadth-first search is performed, which is initialized with the seed genes. During the search, the minimum distance to the seed genes is recorded until seed genes are reachable from one another. Upon completion, the final network is obtained by exploring the shortest paths, starting from the seed genes, that have a maximum length of 4 and that connect at least two seed genes. Hence, the extracted network is made of one or more connected components and may not include all the seed genes. The obtained networks were visualized using Cytoscape [40].

Acknowledgements

Special thanks to Robin Hiesinger for stimulating discussions. We thank H. J. Bellen, the Developmental studies Hybridoma Bank and the VDRC for flies and antibodies. We especially thank A. P. Jarman for sharing the unpublished *ato* RNAi lines and Juan Modolell for the *UAS::sc* flies. This work was supported by an FWO postdoctoral fellowship to S.A., VIB, Impuls, CREA and GOA grants from K.U. Leuven, and FWO grant number G.0542.08N, to B.A.H. and the following grants to Y.M.: GOA AMBioRICS, CoE EF/05/007 SymBioSys, PROMETA, FWO (G.0241.04, G.0499.04, G.0232.05, G.0318.05, G.0553.06, G.0302.07, ICCoS, ANMMM, MLDM), IWT (GBOU-McKnow-E, GBOU-ANA, TAD-BioScope-IT, Silicos, SBO-BioFrame, SBO-MoKa, TBM-Endometriosis, TBM-IOTA3), IUAP P6/25, ERNSI, FP6-NoE Biopattern, FP6-IP e-Tumours, FP6-MC-EST Bioptrain, FP6-STREP Strokemap.

References

1. Adie EA, Adams RR, Evans KL, Porteous DJ, Pickard BS (2006) SUSPECTS: enabling fast and effective prioritization of positional candidates. Bioinformatics 22: 773-774.

2. Aerts S, Lambrechts D, Maity S, Van Loo P, Coessens B, et al. (2006) Gene prioritization through genomic data fusion. Nat Biotechnol 24: 537-544.

3. Freudenberg J, Propping P (2002) A similarity-based method for genome-wide prediction of disease-relevant human genes. Bioinformatics 18 Suppl 2: S110-115.

4. George RA, Liu JY, Feng LL, Bryson-Richardson RJ, Fatkin D, et al. (2006) Analysis of protein sequence and interaction data for candidate disease gene prediction. Nucleic Acids Res 34: e130.

5. Lopez-Bigas N, Ouzounis CA (2004) Genome-wide identification of genes likely to be involved in human genetic disease. Nucleic Acids Res 32: 3108-3114.

6. Ma X, Lee H, Wang L, Sun F (2007) CGI: a new approach for prioritizing genes by combining gene expression and protein-protein interaction data. Bioinformatics 23: 215-221.

7. Oti M, Snel B, Huynen MA, Brunner HG (2006) Predicting disease genes using protein-protein interactions. J Med Genet 43: 691-698.

8. Perez-Iratxeta C, Bork P, Andrade-Navarro MA (2007) Update of the G2D tool for prioritization of gene candidates to inherited diseases. Nucleic Acids Res.

9. Rossi S, Masotti D, Nardini C, Bonora E, Romeo G, et al. (2006) TOM: a web-based integrated approach for identification of candidate disease genes. Nucleic Acids Res 34: W285-292.

10. Tiffin N, Adie E, Turner F, Brunner HG, van Driel MA, et al. (2006) Computational disease gene identification: a concert of methods prioritizes type 2 diabetes and obesity candidate genes. Nucleic Acids Res 34: 3067-3081.

11. Tiffin N, Kelso JF, Powell AR, Pan H, Bajic VB, et al. (2005) Integration of text- and data-mining using ontologies successfully selects disease gene candidates. Nucleic Acids Res 33: 1544-1552.

12. van Driel MA, Cuelenaere K, Kemmeren PP, Leunissen JA, Brunner HG, et al. (2005) GeneSeeker: extraction and integration of human disease-related information from web-based genetic databases. Nucleic Acids Res 33: W758-761.

13. Guillemot F (1999) Vertebrate bHLH genes and the determination of neuronal fates. Exp Cell Res 253: 357-364.

14. Campuzano S, Modolell J (1992) Patterning of the Drosophila nervous system: the achaete-scute gene complex. Trends Genet 8: 202-208.

15. Anderson DJ (1999) Lineages and transcription factors in the specification of vertebrate primary sensory neurons. Curr Opin Neurobiol 9: 517-524.

16. Brunet JF, Ghysen A (1999) Deconstructing cell determination: proneural genes and neuronal identity. Bioessays 21: 313-318.

17. Jan YN, Jan LY (1994) Neuronal cell fate specification in Drosophila. Curr Opin Neurobiol 4: 8-13.

18. Cabrera CV, Alonso MC (1991) Transcriptional activation by heterodimers of the achaete-scute and daughterless gene products of Drosophila. Embo J 10: 2965-2973.

19. Hassan BA, Bellen HJ (2000) Doing the MATH: is the mouse a good model for fly development? Genes Dev 14: 1852-1865.

20. Vervoort M, Ledent V (2001) The evolution of the neural basic Helix-Loop-Helix proteins. ScientificWorldJournal 1: 396-426.

21. Quan XJ, Hassan BA (2005) From skin to nerve: flies, vertebrates and the first helix. Cell Mol Life Sci 62: 2036-2049.

22. Hiesinger PR, Hassan BA (2005) Genetics in the age of systems biology. Cell 123: 1173-1174.

23. Quan XJ, Denayer T, Yan J, Jafar-Nejad H, Philippi A, et al. (2004) Evolution of neural precursor selection: functional divergence of proneural proteins. Development 131: 1679-1689.

24. Skowronska-Krawczyk D, Matter-Sadzinski L, Ballivet M, Matter JM (2005) The basic domain of ATH5 mediates neuron-specific promoter activity during retina development. Mol Cell Biol 25: 10029-10039.

25. St Johnston D (2002) The art and design of genetic screens: Drosophila melanogaster. Nat Rev Genet 3: 176-188.

26. Kanehisa M, Goto S, Kawashima S, Okuno Y, Hattori M (2004) The KEGG resource for deciphering the genome. Nucleic Acids Res 32: D277-280.

27. Arbeitman MN, Furlong EE, Imam F, Johnson E, Null BH, et al. (2002) Gene expression during the life cycle of Drosophila melanogaster. Science 297: 2270-2275.

28. Li TR, White KP (2003) Tissue-specific gene expression and ecdysone-regulated genomic networks in Drosophila. Dev Cell 5: 59-72.

29. Tomancak P, Beaton A, Weiszmann R, Kwan E, Shu S, et al. (2002) Systematic determination of patterns of gene expression during Drosophila embryogenesis. Genome Biol 3: RESEARCH0088.

30. Hoffmann R, Valencia A (2004) A gene network for navigating the literature. Nat Genet 36: 664.

31. Boyle EI, Weng S, Gollub J, Jin H, Botstein D, et al. (2004) GO::TermFinder--open source software for accessing Gene Ontology information and finding significantly enriched Gene Ontology terms associated with a list of genes. Bioinformatics 20: 3710-3715.

32. Friedman A, Perrimon N (2007) Genetic screening for signal transduction in the era of network biology. Cell 128: 225-231.

33. Jarman AP, Sun Y, Jan LY, Jan YN (1995) Role of the proneural gene, atonal, in formation of Drosophila chordotonal organs and photoreceptors. Development 121: 2019-2030.

34. Jarman AP, Grell EH, Ackerman L, Jan LY, Jan YN (1994) Atonal is the proneural gene for Drosophila photoreceptors. Nature 369: 398-400.

35. Vaessin H, Grell E, Wolff E, Bier E, Jan LY, et al. (1991) prospero is expressed in neuronal precursors and encodes a nuclear protein that is involved in the control of axonal outgrowth in Drosophila. Cell 67: 941-953.

36. Lage P, Jan YN, Jarman AP (1997) Requirement for EGF receptor signalling in neural recruitment during formation of Drosophila chordotonal sense organ clusters. Curr Biol 7: 166-175.

37. Dietzl G, Chen D, Schnorrer F, Su KC, Barinova Y, et al. (2007) A genome-wide transgenic RNAi library for conditional gene inactivation in Drosophila. Nature 448: 151-156.

38. von Mering C, Jensen LJ, Kuhn M, Chaffron S, Doerks T, et al. (2007) STRING 7--recent developments in the integration and prediction of protein interactions. Nucleic Acids Res 35: D358-362.

39. Mardon G, Solomon NM, Rubin GM (1994) dachshund encodes a nuclear protein required for normal eye and leg development in Drosophila. Development 120: 3473-3486.

40. Shannon P, Markiel A, Ozier O, Baliga NS, Wang JT, et al. (2003) Cytoscape: a software environment for integrated models of biomolecular interaction networks. Genome Res 13: 2498-2504.

Figure Legends

Figure 1: Overexpression of Ngn^{bato} in the *sense* mutant background provides a robust and sensitive phenotype for screening of *ato* dependent enhancers and suppressors. (A) Amino Acid sequence of the basic domain of Ngn (green) and Ato (red). The functionally critical amino acids are shown in separate colors. (B) Bristle phenotype on the third wing vein induced by Ngn^{bato} driven by dpp-Gal4. (C) Quantitative assay of ectopic bristle formation induced by Ngn^{bato} in wild type, *sens/+*, *da/+;sens/+* and *N/+; sens/+* backgrounds. Ato and Ngn are shown as positive and negative controls, respectively. Removing one copy of senseless reduces the amount of ectopic bristles. Removing one copy of *da* in a *sens/+* background results in a suppression of the phenotype, whereas removing one copy of *N* results in an enhancement of the phenotype. (D) Cytological position of the deficiency regions and amount of genes found within each atonal positive deficiency region on chromosome 2 and chromosome 3.

Figure 2: HIGHFLY Cross-validation results.

The AUC performance values obtained for all individual data sources (on the x-axis) are shown for several validation sets (each validation set is plotted in a different color; see legend). The AUC values for the overall prioritization, obtained by integrating all individual rankings, are also shown.

Figure 3: Ranking specificity of the *ato* interacting genes in the bristle assay. The observed rank of a positive gene, using the Atonal specific training set is compared to its rank obtained with a random training set (100 times). Shown is a boxplot of the 100 "random" rankings of

each positive gene (y axis). The green asterisk represents the rank of the positive for the Atonal training set.

Figure 4: Distribution of the phenotypic range of the average number of bristles per genotype (n > 10) plotted for all ~600 assayed genotypes (y-axis). The shape of the curve conforms to the expectations for quantitative screens [32].

Figure 5: Effect of modifiers on eye size in atonal sensitized eyes

A) wild type eye with around 800 ommatidia, (B) effect from *ato-RNAi* on amount of ommatidia resulting in a population of flies with 400 ommatidia per eye, (C) enhancement of *ato-RNAi* phenotype resulting in a population with smaller eyes with 250 ommatidia per eye. (D) overview of phenotypes observed when modifiers were crossed with atoRNAi flies, removal of one copy of the modifier results in a larger population of flies with smaller eyes for 8 of the previously identified modifiers. The other 4 modifiers didn't show an alteration in eye phenotype, compared to the *ato-RNAi* phenotype in controls.

Figure 6: Protein-protein association subnetworks.

The subgraphs are extracted from STRING connections with score above 0.842, and aim to connect as many seed genes as possible. Seed genes may be connected through maximally two edges from either side. (A) The 16 positive 'known' genes are used a seed genes to validate their potential relationship. The resulting network is significantly larger and more interconnected than expected by chance and recovers Ato itself as member of the sub-network. (B) Example of a subgraph generated from a random selection of seed genes that does recover Ato. Only 29 out of 1000 random networks recover Ato by chance. These networks are significantly smaller than the network formed by the 16 genes from the screen.

Figure 7: Comparison of whole-genome prioritizations for signaling pathways with results from RNAi screens obtained from http://www.flyrnai.org. For each of the four prioritizations the training set is based on Gene Ontology annotation for the respective pathway, namely GO:0000165 (MAPK) for the ERK pathway (A), GO:0007259 for JAK-STAT (B), GO:00016055 for Wnt (C), and GO:0007224 (smoothened) for hh (D). The green curve represents the cumulative recovery of positive genes when moving down the top 10% of the ranked gene list, using the full training set. The orange curve is similar to the green curve, but now excluding the known GO-annotated positives from the RNAi screen from the training set. The blue control curve is the average recovery curve of the positives, using 100 random training sets of known GO-annotated genes. The grey area represents a 95% confidence interval above the mean and the dotted curve represents two standard deviations above the mean, so that every point above the dotted curve represents a significant ($p<0.05$) enrichment of true positives. For three out of four, namely ERK, Wnt and JAK-STAT, a significant enrichment of positives is found at nearly all thresholds in the top 10% of the genome.

Table 1. HIGHFLY training and scoring strategies for each data source.

Table 2. Validation of HIGHFLY on prioritized 3R chromosome and on different prioritized deficiency regions. Rank on prioritized list of each positive gene is given within the prioritized region and within the overall chromosome prioritization.

Table 3. Enrichment of GO-terms for the results of the screen.

Table 4. Top 10% ranking genes in each deletion prioritized by HIGHFLY.

Table 5. Synthetic lethal modifiers of *ato-RNAi* among the unknown genes.

A

Amino acid sequence of basic domain

ATO: RRLAANARERRR

NGN: RRVKANDRERNR

NGNbATO: RRVAANARERRR

B

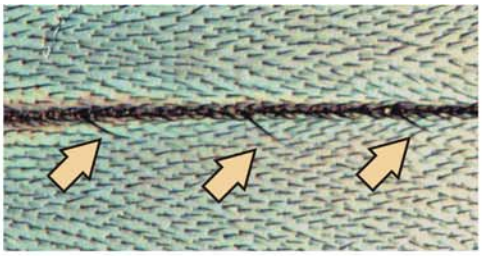

UASngnbato/+;dppGal4/+

C

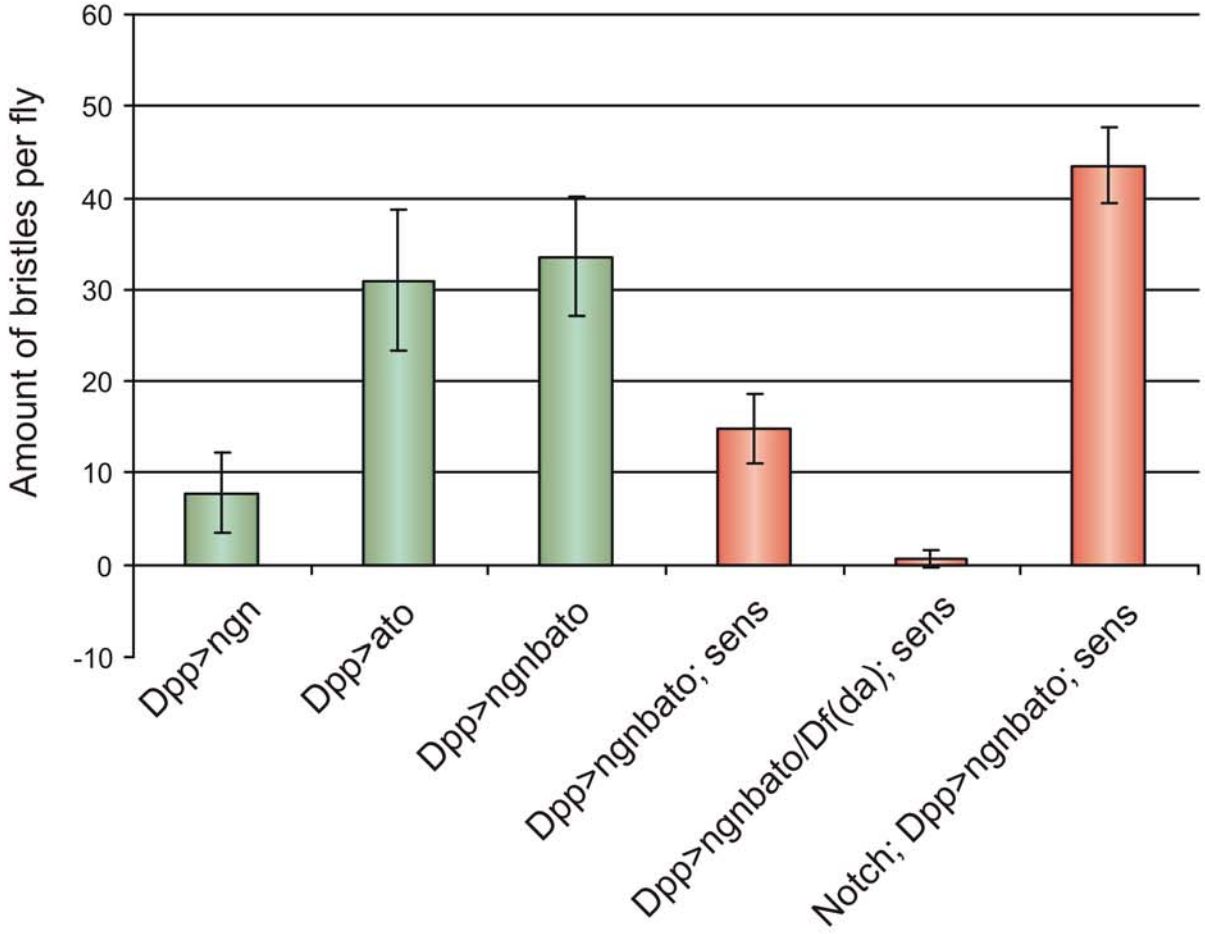

D

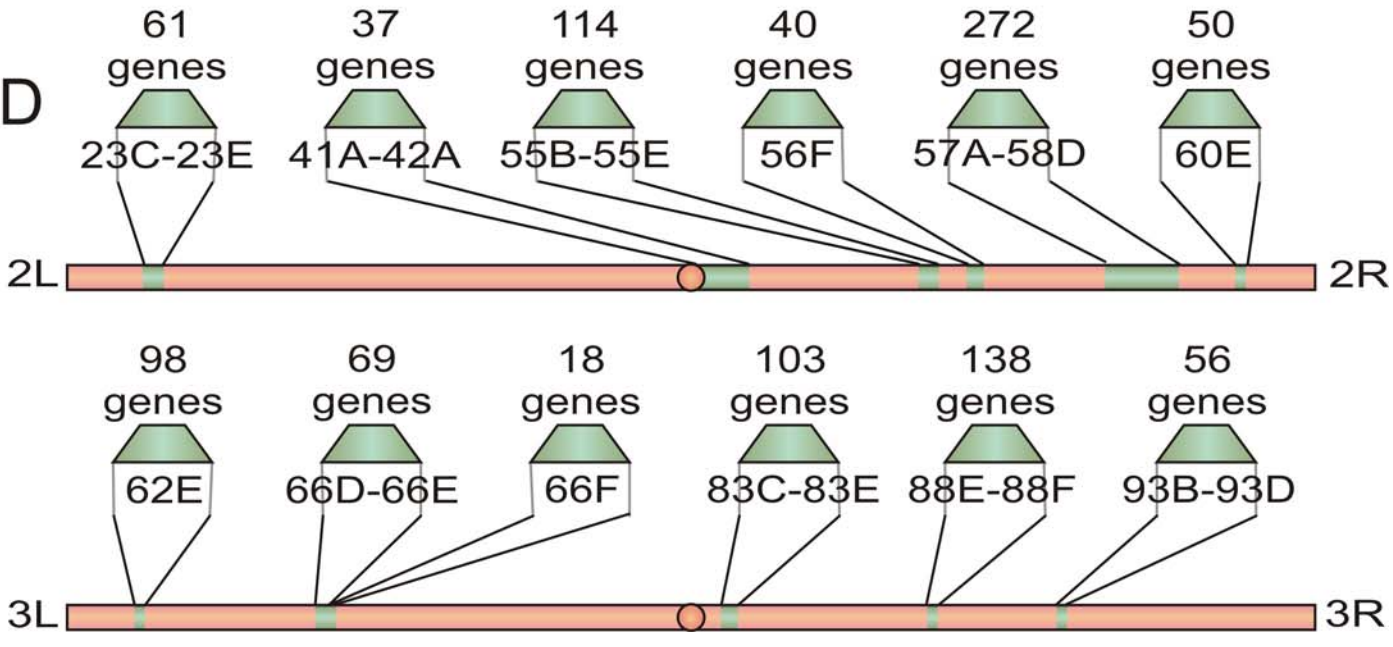

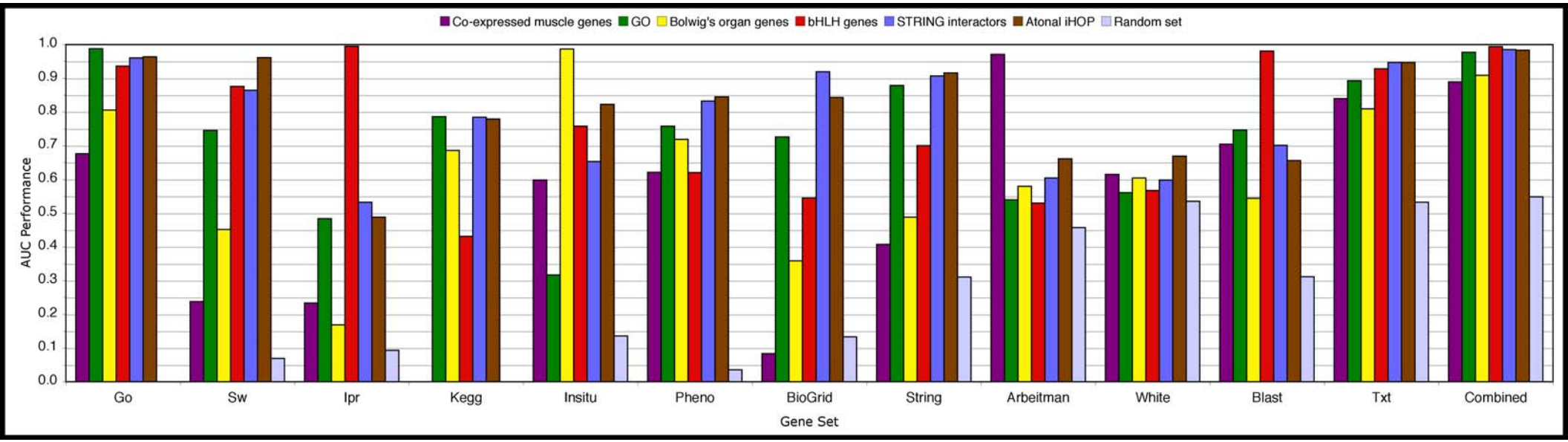
Co-expressed muscle genes
GO
Bolwig's organ genes
bHLH genes
STRING interactors
Atonal iHOP
Random set
AUC Performance
1.0
0.9
0.8
0.7
0.6
0.5
0.4
0.3
0.2
0.1
0.0
Go
Sw
Ipr
Kegg
Insitu
Pheno
BioGrid
String
Arbeitman
White
Blast
Txt
Combined
Gene Set

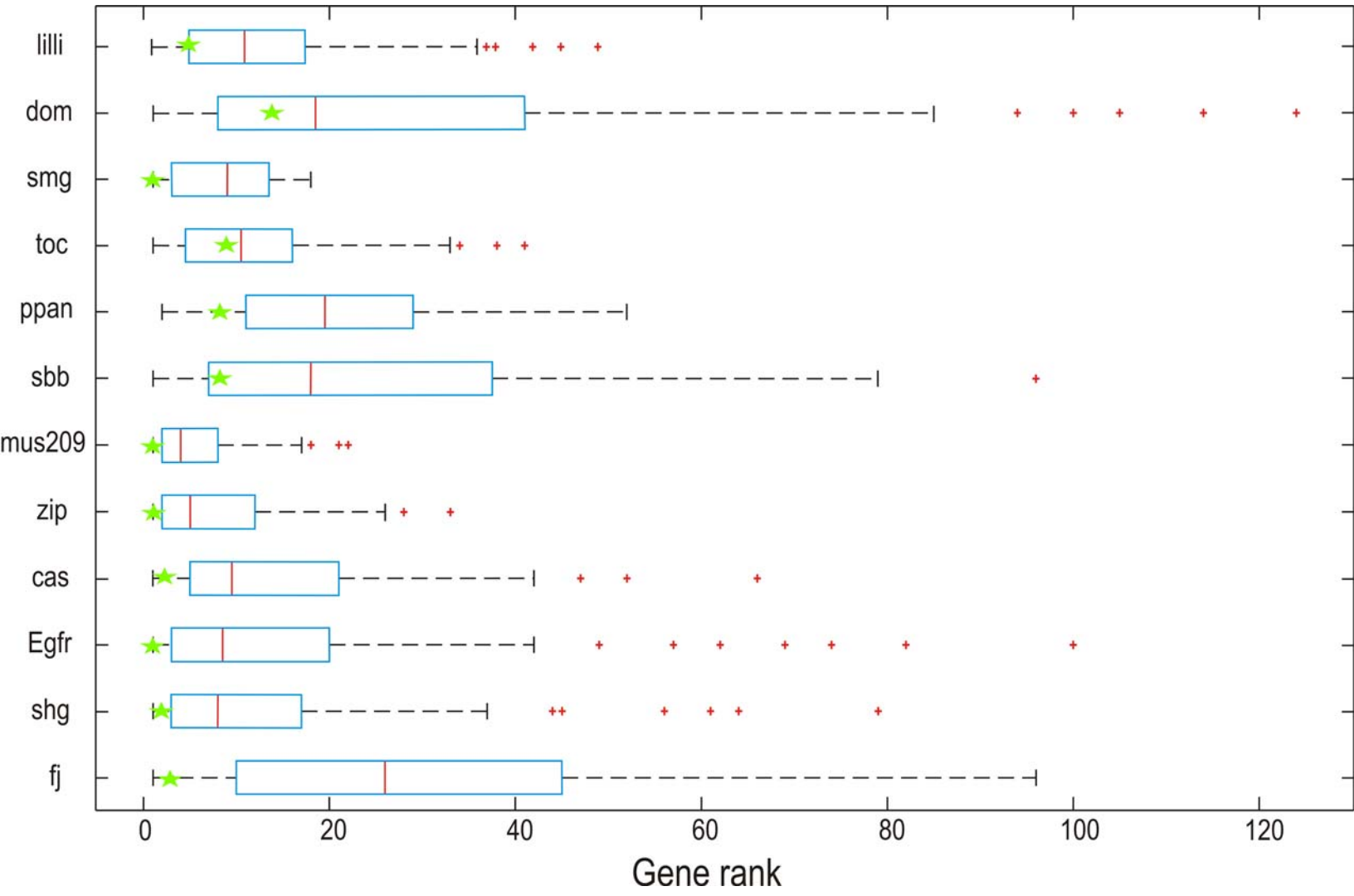
lilli
dom
smg
toc
ppan
sbb
mus209
zip
cas
Egfr
shg
fj
0
20
40
60
80
100
120
Gene rank

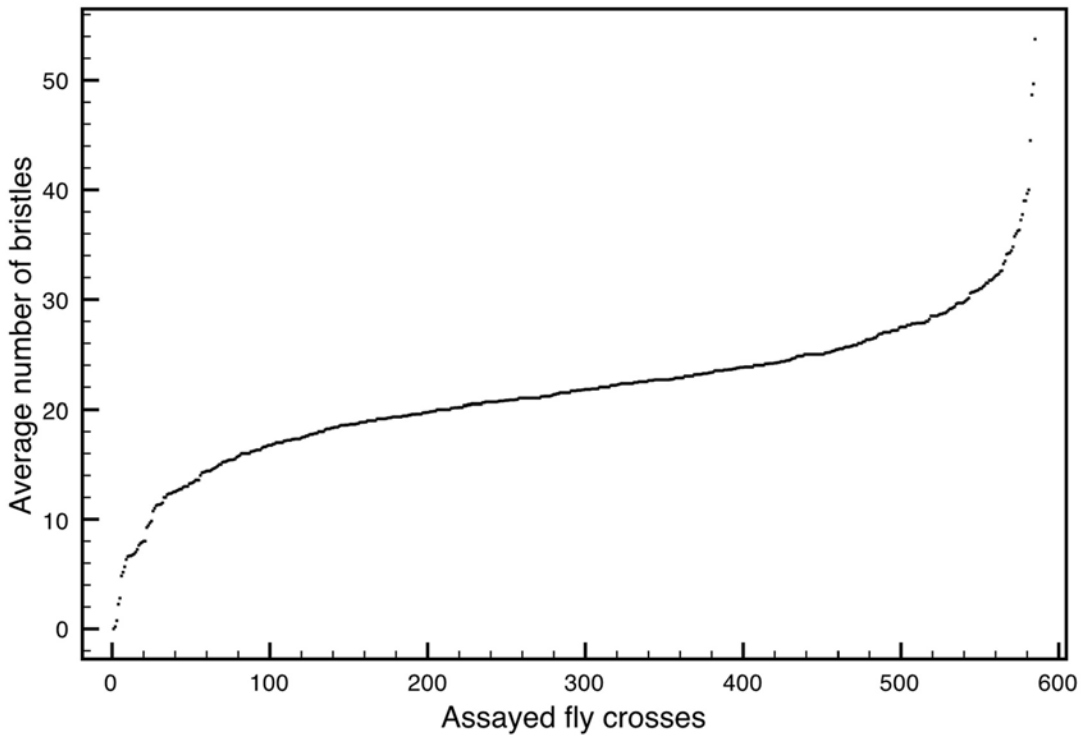
Average number of bristles
0
10
20
30
40
50
0
100
200
300
400
500
600
Assayed fly crosses

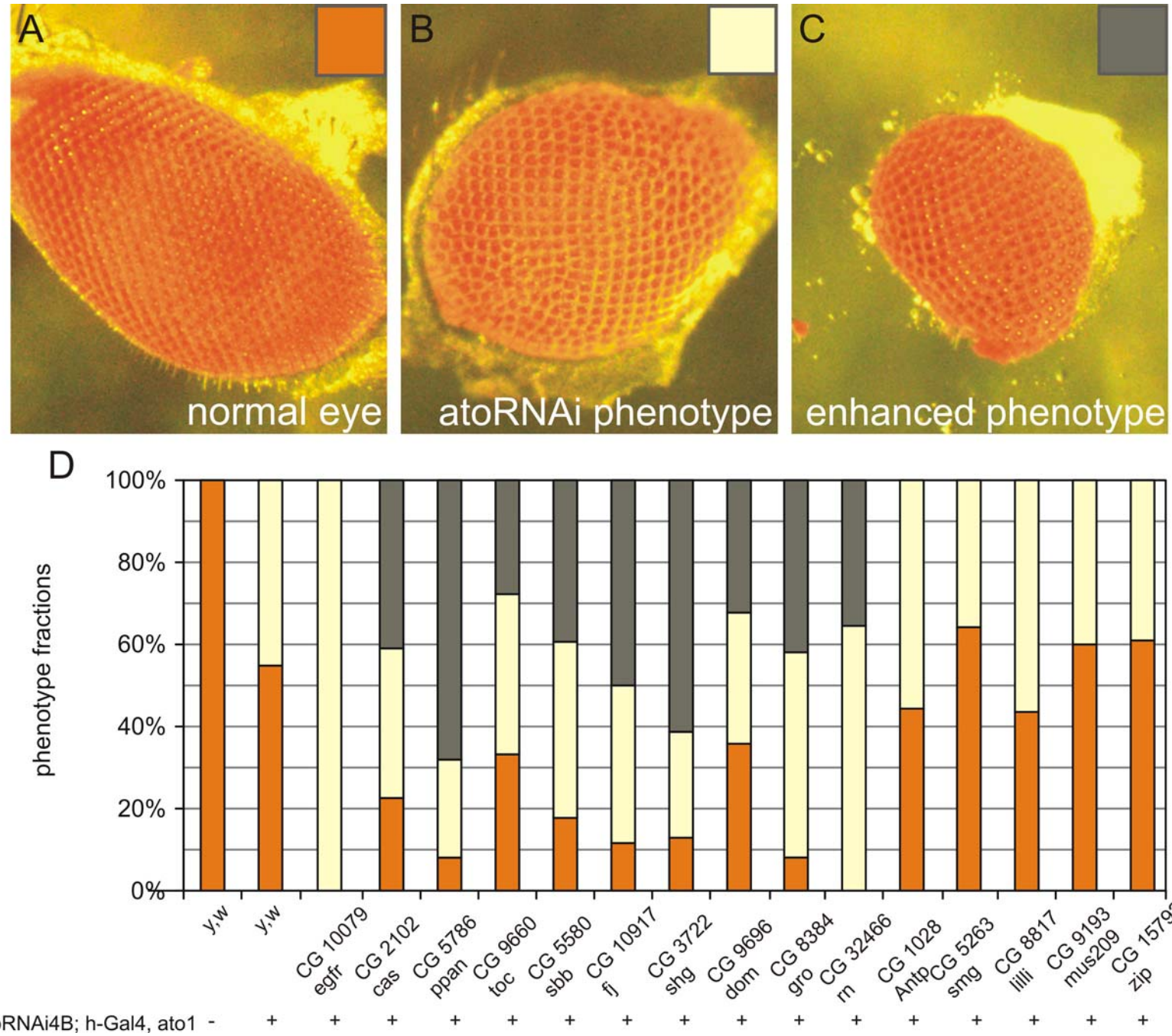
A
normal eye
B
atoRNAi phenotype
C
enhanced phenotype
D
phenotype fractions
100%
80%
60%
40%
20%
0%
y,w
y,w
CG 10079
egfr
CG 2102
cas
CG 5786
ppan
CG 9660
toc
CG 5580
sbb
CG 10917
fj
CG 3722
shg
CG 9696
dom
CG 8384
gro
CG 32466
rn
CG 1028
Antp
CG 5263
smg
CG 8817
lilli
CG 9193
mus209
CG 15792
zip
AtoRNAi4B; h-Gal4, ato1 - + + + + + + + + + + + + + + + + +

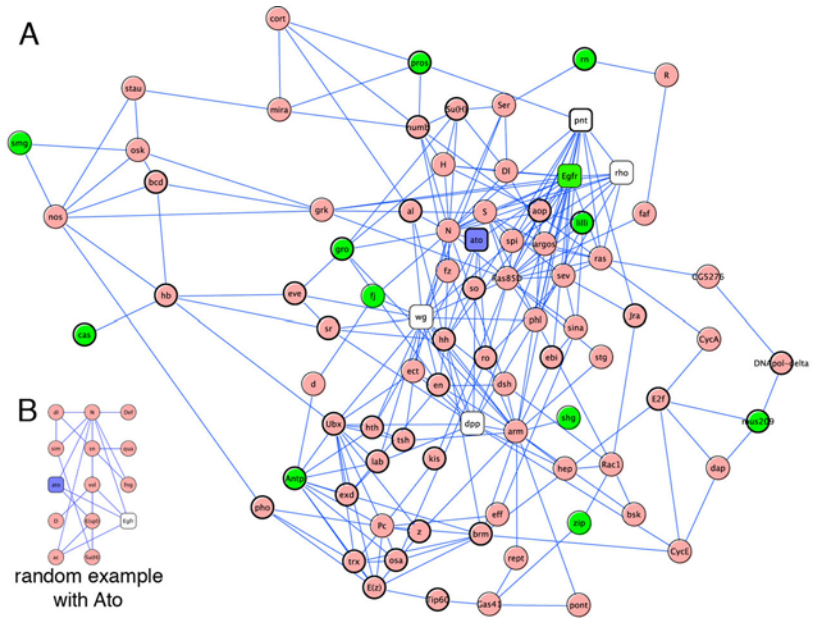
A
B
random example
with Ato
cort
pros
rn
R
stau
mira
Su(H)
Ser
pnt
smg
osk
numb
H
Dl
Egfr
rho
bcd
nos
grk
al
S
aop
faf
N
ato
spi
argos
lilli
gro
ras
fz
Ras85D
sev
CG5276
hb
eve
fj
so
wg
phl
sina
Jra
cas
sr
hh
CycA
ro
ebi
stg
DNApol-delta
ect
en
dsh
d
E2f
Ubx
hth
dpp
arm
shg
mus209
tsh
lab
kis
hep
Rac1
dap
Antp
exd
pho
eff
bsk
Pc
z
brm
zip
CycE
trx
osa
rept
E(z)
Tip60
Gas41
pont

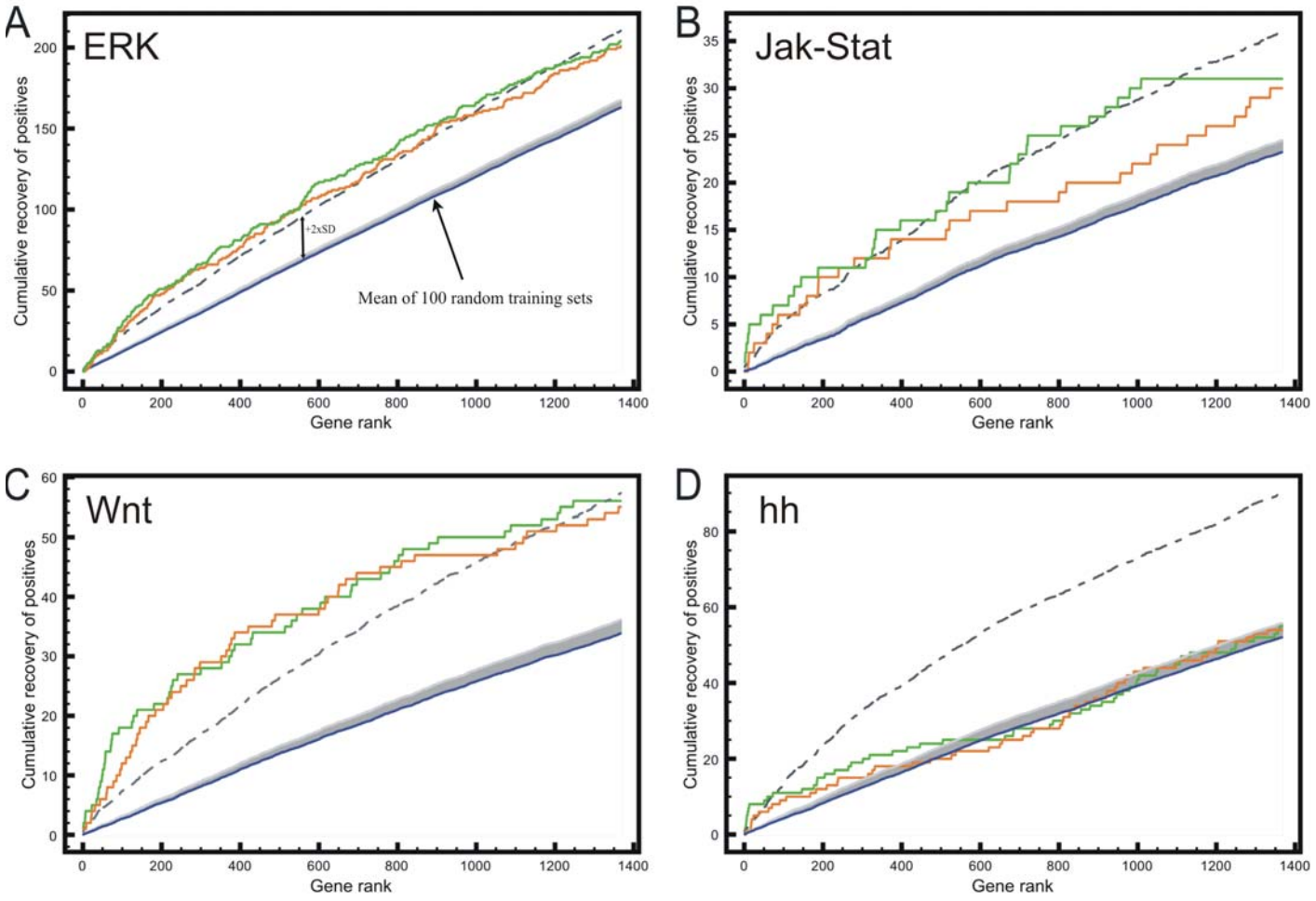

: Overlap of HighFly prioritizations, using pathway GO terms, with positive genes from siRNA screen

: Overlap of HighFly prioritizations, using pathway GO terms minus overlap genes, with positive genes from siRNA scre

Table1. Highfly data sources

Data type	Data source	Training	Scoring
Functional annotation	Gene Ontology	GO term over-representation	Fisher's omnibus
	PubMed abstract profiles	Text-mining using gene-reference relations from FlyBase; average term weight vector	Cosine similarity
	SwissProt keywords	Term over-representation	Fisher's omnibus
	KEGG [26]	Pathway over-representation	Fisher's omnibus
Gene expression	Life cycle of Drosophila microarray data [27]	Collection of all the expression profiles of the training genes	Average of 50% best Pearson correlation
	Tissue-specific gene expression in Drosophila larvae [28]	Collection of all the expression profiles of the training genes	Average of 50% best Pearson correlation
	In situ expression [29]	FBbt term over-representation	Fisher's omnibus
Protein sequence	InterPro	Domain over-representation	Fisher's omnibus
	BLAST	Ad hoc BLAST database of training genes prot. seq.	Blast test seq. to ad hoc db; rank by e-value
Allele phenotypes	FlyBase records "phenotype manifest in"	FBbt term over-representation	Fisher's omnibus
Genetic interactions and protein interactions	BioGrid	List of training genes and all their interactors	Overlap between the test gene plus its interactors and the training list
	STRING [38]	Idem BioGrid	Idem BioGrid

Table2. Validation of the HIGHFLY screen results

name	Flybase ID	chromosome	rank on test region	rank ratio on test region	rank on chromosome	rank ratio on chromosome	phenotype	P-Value
Antp	FBgn0000095	chr3	44/3341	1.31%	67/6027	1.10%	-31.40%	<0.001
gro	FBgn0001139	chr3	58/3341	1.74%	84/6027	1.40%	-69.90%	<0.001
pros	FBgn0004595	chr3	33/3341	0.99%	48/6027	0.80%	dead	
rn	FBgn0003263	chr3	13/3341	0.39%	21/6027	0.40%	44.20%	<0.001
cas	FBgn0004878	chr3	2/103	1.94%	123/6027	2.00%	-33.60%	<0.001
dom	FBgn0020306	chr2	14/272	5.15%	413/5252	7.90%	-31.40%	<0.002
Egfr	FBgn0003731	chr2	1/272	0.37%	2/5252	0.03%	-51.30%	<0.001
fj	FBgn0000658	chr2	3/114	2.63%	63/5252	1.20%	-50.00%	<0.001
lilli	FBgn0041111	chr2	5/61	8.20%	245/5252	4.70%	-35.40%	<0.002
mus209	FBgn0005655	chr2	1/40	2.50%	484/5252	9.20%	-36.70%	<0.005
ppan	FBgn0010770	chr3	8/56	14.29%	642/6027	10.70%	-33.60%	<0.002
sbb	FBgn0010575	chr2	8/114	7.02%	207/5252	3.90%	-33.60%	<0.001
shg	FBgn0003391	chr2	2/272	0.74%	30/5252	0.60%	-66.40%	<0.001
smg	FBgn0016070	chr3	1/18	5.56%	279/6027	4.60%	-100%	<0.001
toc	FBgn0015600	chr2	9/61	14.75%	834/5252	15.90%	-33.60%	<0.001
zip	FBgn0005634	chr2	1/50	2.00%	123/5252	2.30%	-38.10%	<0.001

Table 3: Selection of enriched GO-terms across the 16 positive genes. Full results table is available at http://med.kuleuven.be/cme-mg/lng/HighFly. All genes from chr2 and chr3 are used as background set.

GO ID	Genes	Group count	Total count	P value	GO term
GO:0007444	*rn*; *pros*; *lilli*; *fj*; *ppan*; *EGFR*	6	259	0.000214	imaginal disc development
GO:0046530	*pros*; *lilli*; *sbb*; *EGFR*	4	72	0.000255	photoreceptor cell differentiation
GO:0016477	*zip*; *shg*; *dom*; *sbb*; *EGFR*	5	160	0.000276	cell migration
GO:0000904	*pros*; *lilli*; *shg*; *sbb*; *EGFR*	5	162	0.000284	cell differentiation
GO:0003700	*rn*; *cas*; *pros*; *lilli*; *Antp*; *sbb*	6	314	0.000447	transcription factor activity
GO:0007417	*cas*; *pros*; *shg*; *EGFR*	4	95	0.000622	central nervous system development
GO:0007420	*cas*; *shg*; *EGFR*	3	34	0.000693	brain development
GO:0007560	*rn*; *pros*; *lilli*; *fj*; *EGFR*	5	210	0.000764	imaginal disc morphogenesis
GO:0035218	*rn*; *fj*; *EGFR*	3	37	0.000811	leg disc development
GO:0001745	*pros*; *lilli*; *fj*; *EGFR*	4	108	0.000811	compound eye morphogenesis
GO:0007164	*fj*; *zip*; *EGFR*	3	38	0.000811	establishment of tissue polarity
GO:0000278	*zip*; *ppan*; *toc*; *mus209*; *EGFR*	5	223	0.000811	mitotic cell cycle

Table 4: Top 10% ranking genes in each deletion prioritized by HIGHFLY

Deleted region	Uncovered Genes
23C-23E	*CG3277*, *Mad*, *CG3485*, *CG18555*, *lilli*
41A-42A	*src42A*, *CG30431*, *EcR*
55B-55E	*Pcl, edl, fj*, *Hsf*, *lolal*, *Idgf5*, *stau*, *sbb*, *CG5733*, *CG15072*, *CG5335*
56F	*mus209*, *CG11788*, *CG13871*
57A-58D	*Egfr*, *shg*, *insc*, *cv-2*, *bl*, *tud*, *grau*, *Tbp*, *PTP-ER*, *Gp150*, *CG30281*, *dve*, *otp*, *dom*, *CG3216*, *CG11110*, *CG10543*, *Fkbp13*, *Sdc*, *rig*, *Rx*, *ari-2*, *CG10955*, *mago*, *CG3624*, *Xbp1*
60E	*zip*, *CG2790*, *Dll*, *key*
62E	*msn*, *FR*, *dos*, *Hsp83*, *CG1244*, *CG16753*, *Mrtf*, *Spn*, *CG32295*, *rasp*
66D-66E	*h*, *dally*, *foi*, *CG13309*, *CG6765*, *CG6416*
66F	*smg*
83C-83E	*Pak*, *cas*, *CG10979*, *NPFR1*, *CG10267*, *CG1218*, *CG1024*, *CG9727*, *TfIIFalpha*
88E-88F	*CG9593*, *pnr*, *srp*, *Hsc70-4*, *Rh6*, *Tm1*, *ea*, *tefu*, *CG6654*, *Sra-1*, *Su(var)3-9*, *CG31392*, *Art3*
93B-93D	*Tin*, *mod(mdg4)*, *ETHR, bap*, *SIFR*

Table 5: Results of the phenotypes observed from RNAi screen					
clone	CG number	Rank	CG-RNAi + atoRNA ;hGal4, ato[1]	CGRNAi + hGal4, ato[1]	CGRNAi + hGal4
18597	*CG1024*	7.7%	Lethal	No Effect	No Effect
31685	*CG1218*	6.6%	Lethal	No Effect	No Effect